

Original Research

Pd-Cu Bimetallic Based Catalysts for Nitrate Remediation in Water: Synthesis, Characterization, and the Influence of Supports

Mouhamad Rachini^{1, 2}, Mira Jaafar^{1, 3}, Fatima Al Ali³, Zahraa Sleiman¹, Mohammad Kassem², Eugene Bychkov², T. Jean Daou^{4, 5}, Joumana Toufaily³, Tayssir Hamieh^{1, 6, *}

1. Laboratory of Materials, Catalysis, Environment and Analytical Methods (MCEMA), EDST, FS, Lebanese University, P.O. Box 11-2806, Hariri Campus, Hadath, Lebanon; E-Mails: mouhamadrachini@outlook.com; mirah.jaafar@ul.edu.lb; zahraa_slaiman@hotmail.com; t.hamieh@maastrichtuniversity.nl
2. Université du Littoral Côte d'Opale (ULCO), LPCA, EA 4493, F-59140 Dunkerque, France; E-Mails: Mohamad.Kassem@univ-littoral.fr; eugene.bychkov@univ-littoral.fr
3. Laboratory of Applied Studies for Sustainable Development and Renewable Energy (LEADDER), EDST, Lebanese University, P.O. Box 11-2806, Hariri Campus, Hadath, Lebanon; E-Mails: alalifatima@yahoo.fr; joumana.toufaily@ul.edu.lb
4. Université de Haute-Alsace (UHA), CNRS, Institut de Science des Matériaux de Mulhouse (IS2M), Axe Matériaux à Porosité Contrôlée (MPC), UMR 7361, 68100 Mulhouse, France; E-Mail: jean.daou@uha.fr
5. Université de Strasbourg, 67000 Strasbourg, France
6. Faculty of Science and Engineering, Maastricht University, P.O. Box 616, 6200 MD, Maastricht, The Netherlands

* **Correspondence:** Tayssir Hamieh; E-Mail: t.hamieh@maastrichtuniversity

Academic Editor: Md Ariful Ahsan

Special Issue: [Applications of Environmental Catalysis](#)

Catalysis Research
2022, volume 2, issue 2
doi:10.21926/cr.2202011

Received: January 29, 2022
Accepted: April 12, 2022
Published: April 21, 2022

Abstract

The use of Pd-Cu bimetallic catalysts in the reduction of aqueous nitrate ions by hydrogen was studied. The catalysts were supported on multi-walled carbon nanotubes (MWCNTs),



© 2022 by the author. This is an open access article distributed under the conditions of the [Creative Commons by Attribution License](#), which permits unrestricted use, distribution, and reproduction in any medium or format, provided the original work is correctly cited.

activated carbon (AC), and Titania, and the influence of the support on the nitrate reduction activity in water was then investigated. The catalysts were characterized before and after use by FT-IR, XRD, SEM, EDX, and Laser Granulometry. It was found that the surface characteristics of the support have an influence on the catalyst activity, with Pd-Cu supported on MWCNT displaying the highest reduction efficiency.

Keywords

Pd-Cu bimetallic catalyst; multi-walled carbon nanotubes (MWCNTs); XRD; BET; SEM; FTIR

1. Introduction

Nitrate and nitrite are naturally occurring ions that play active roles in the nitrogen cycle. However, while nitrogen is essential for all living things as it is a component of protein, excessive concentrations of nitrate-nitrogen in drinking water can be hazardous to health [1]. This problem has become acute, as the intensive use of fertilizers and pesticides has led to the presence of extensive nitrate concentrations in groundwater, which is considered the main source of drinking water [2].

Nitrate is highly soluble, so it readily enters soil and groundwater and can be carried directly into surface water in run-off and field run-off [3]. This has led to nitrate levels in many groundwater bodies and rivers around the world to have increased over the past 50 years. While not directly toxic to the human body, nitrate in an anaerobic state, such as when in the human gut, is converted to nitrite, which can lead to so-called “blue baby syndrome”. Nitrates are also precursors to carcinogenic nitrosamines and other N-nitroso compounds [4].

Many physicochemical processes can be used to remove nitrates from the water, such as ion exchange [5], reverse osmosis [6, 7], electrodialysis [8], or adsorption [9, 10]. However, with all these processes, the nitrates require treatment post-removal to be made harmless [11]. Biological treatment can convert nitrates into harmless nitrogen directly, but such processes (either heterotrophic or autotrophic) introduced handling difficulties and can lead to the release of undesirable biomass or toxic by-products [11]. The third approach to nitrate removal is the reduction of nitrates to nitrogen using hydrogen as a reducing agent over a supported bimetallic catalyst. Several studies have been conducted on this approach following early work by Vorlop et al. [12], all of which follow a general scheme of using a promoter metal or bimetal system (preferably Pd-Cu) that allows nitrate adsorption. Following this adsorption, nitrate is first reduced to nitrite; then nitrite is converted to other intermediates (NO, N₂O), before. Finally, nitrogen is formed as the main product, alongside ammonium, which is an unwanted by-product generated due to excessive hydrogenation [13]. Although this general mechanism suggests that the activity of the noble metals must be enhanced (promoted) by a second metal in the first step of nitrate reduction to nitrite, some studies that have used monometallic catalysts supported on metal oxides such as ceria [14] or Titania [15] to reduce nitrates, and the mechanism includes the partly reduced species of the support. In 1989, Vorlop et al. proposed the catalytic hydrogenation of nitrate over a bimetallic palladium catalyst to remove nitrate from drinking water [12]. In this process, nitrate passes through several steps via NO₂⁻, NO and N₂O intermediates as it is reduced to molecular nitrogen. Ammonia

is also generated as an undesirable by-product, forming from the secondary reaction of hydrogen and NO adsorbed on the catalyst surface. Prüsse et al. [16] proposed a mechanistic model with three principal elements: 1) nitrate reduction occurs primarily at the bimetallic site (Pd-Cu; palladium-tin), 2) nitrite reduction occurs at monometallic sites (Pd), and 3) reaction selectivity is determined by the N/reducer ratio at the single metal site of palladium. According to Prüsse et al., as the promoter metal content increases, the nitrite reduction activity on the bimetallic catalyst decreases [17] - the significant formation of nitrite during the nitrate reduction process supports this conclusion. Later, Illinich et al. [18] proposed an 18-step mechanism for nitrate reduction over supported Pd-Cu bimetallic catalysts. However, the most accepted mechanism is that of Epron et al. [19], who proposed that the promoter metal is responsible for the reduction of NO_3^- by redox reactions, and the primary function of the noble metal (Pd or Pt) is to activate hydrogen, which reduces the promoter metal. Although the noble metals show no activity in reducing NO_3^- , they are very active in the degradation of nitrite (this is thought to occur due to the presence of active hydrogen) [19, 20].

Studies have shown that bimetallic catalysts are more effective than monometallic catalysts [16, 21, 22]. And bimetallic catalysts typically consist of a noble metal (primarily Pd or Pt, but also Ru, Rh, or Ir) and a promoter metal (such as Cu, Sn, Ag, Ni, Fe, or In) deposited on different supports. Pd-Cu, Pd-Sn, and Pt-Cu appear to be the most efficient combinations, but the metals alone are insufficient in their selectivity to nitrogen [23, 24]. To increase their selectivity, they are usually deposited on a support. Many support materials have been used, including alumina [16, 25-27], silica [28, 29], Titania [30], activated carbon [29-32], ceria [14], tin oxide [33], polymers [34], zirconia [35], and alumina membranes [36].

Carbon materials and titanium dioxides have proved to be particularly good supports for nitrate reduction. Yoshinaga et al. [37] reported that Pd-Cu catalysts supported on activated carbon were highly selective to nitrogen, with activities that were higher than those supported on silica or alumina. Similarly, Gao et al. [13] reported that Pd-Cu catalysts supported on TiO_2 were much more active than those supported on Al_2O_3 . While Sá et al. [15] found that palladium supported on titania was also active for this reaction. Nitrate is adsorbed at the exposed Lewis acid sites (oxygen vacancies) of the support via electrostatic interactions, such that, for example, electrons associated with the reduction process can be located at the Ti^{3+} center of Titania supports. However, Pd catalysts supported on TiO_2 have very low nitrogen selectivity, as shown by the strong hydrogenation properties of this catalyst, which lead to over-reduction. However, according to Soares et al. [38], titanium dioxide provides high activity for nitrate reduction, and the use of composites with carbon nanotubes significantly improves selectivity for nitrogen.

In general, carbon materials are good supports for this process, and, consequently, activated carbon (AC) is one of the most used materials in adsorption and catalysis. This is due to many factors: their high surface areas and pore volume, the variety of surface chemical properties that they have, the rapid recovery of supported metal by simple combustion of the support, and the chemical inertness both in acidic and basic media [33-35]. Carbon nanotubes (CNTs) have also attracted attention as a new support in heterogeneous catalysis due to several unique properties [39, 40, 41]. Combined with the ability to attach (functionalize) essentially any chemical species to their sidewalls, the use of CNTs creates opportunities for unique catalyst supports whose electrical conductivity can also be used to find new catalysts and catalytic behaviors. Supporting transition metal nanoparticles on CNTs for catalytic reactions leads to simple product separation, high atomic efficiency, and ease

of catalyst recovery [42]. CNTs offer several advantages over traditional supports, in that, they have a high degree of flexibility in dispersing active phases because their specific surface area or inner diameter can be adjusted, it is easy to chemically functionalize their surfaces and change their chemical composition, and they can catalyze phase deposits on both their outer surface and their inner cavities [43]. Salomé et al. [40] studied the activity and selectivity of Pd-Cu, and Pt-Cu bimetallic catalysts on different carbon material supports for the reduction of nitrate in water. They found by comparing the different supports under the same conditions that carbon nanotubes were the best support. This may be due to the interaction between the precursor and the support during impregnation, which could affect the size of the metallic particles.

Although the focus of the above review has been the role of the support, it must also be acknowledged that several other factors play a role in the activity and selectivity of nitrate reduction, such as the reaction conditions, catalyst preparation, how the noble metals are promoted, etc. [44].

The aim of this present study was to investigate the use of multi-walled carbon nanotubes (MWCNTs), activated carbon, and titania as supports for Pd-Cu bimetallic catalysts for nitrate reduction in water using hydrogen as a reducing agent. The catalyst preparation conditions, catalyst characterization, as well as the effect of the support and pH on the activity of the catalyst, were considered.

2. Experimental

2.1 Materials

The supports used in this study were multi-walled carbon nanotubes (MWCNTs) (70-80%), Activated carbon (AC), and titanium oxide (Titania, TiO₂), purchased from Sigma-Aldrich. TiO₂ and AC were used as received. However, the MWCNTs were purified and functionalized before use. Nitric acid (69%), palladium chloride (99%), copper nitrate (99%), potassium nitrate (≥99%), and sodium borohydride (≥96%), purchased from Sigma-Aldrich, were used in the preparation of the Pd-Cu supported catalysts. Acetonitrile (99.85%) from Scharlau was used as the solvent. While chloroform (99.0-99.4%), potassium sodium tartrate tetrahydrate (99%), sodium salicylate (99.5%), sulfuric acid (98%), purchased from Sigma-Aldrich, and sodium hydroxide (99%), purchased from Riedel-de Haën, were used in the nitrate coloration.

2.2 Purification and Functionalization of the Carbon Nanotubes

The MWCNTs were first heated at 350 °C for 30 min to remove amorphous carbon [45]. Then they were functionalized by using one of two approaches:

2.2.1 Oxidation of the MWCNTs by 8 M Nitric Acid with sonication

The MWCNTs (200 mg) were first sonicated in 8 M nitric acid solution (200 mL) for 1, 2, and 3 h at 40-50 °C to oxidize their surfaces [46], and then filtered and washed with deionized water until a neutral pH was reached [45], before, finally, being dried at 80 °C for 24 h [47, 48].

2.2.2 Oxidation of the MWCNTs by 3 M Nitric Acid at Reflux

The MWCNTs (80 mg) were transferred to a round-bottom flask containing 100 mL of 3 M nitric acid and equipped with a magnetic stirrer bar and a reflux condenser. Then the flask was immersed in an oil bath at 120 °C. The mixtures were heated at reflux for 3 h, cooled to room temperature, and then filtered before. Finally, the solid filtrate was washed with water until the pH became neutral [46].

2.3 Catalyst Preparation

The same procedure was used for all the supports used in this work. The catalysts were first prepared by co-impregnating each support in a mixture of deionized water and acetonitrile (V/V, 3:1) with PdCl₂ and Cu(NO₃)₂ in the required amounts to obtain 4 wt.% Pd - 1 wt.% Cu catalyst. Then NaBH₄ was added dropwise to the solution. After sonication at 65 °C for 1 h, the mixture was filtered and washed several times with deionized water to completely remove any remaining reducing agents before; finally, the solid filtrate was dried at room temperature for several days under vacuum.

2.4 Catalyst Characterization

X-Ray Diffraction (XRD) was used to identify the crystalline phases and purities of the different supports and to confirm the deposition of Pd and Cu metals onto them. The XRD patterns were recorded using a Bruker D8 Advance diffractometer operating in the reflection mode with Cu K α (λ = 0.154056 nm) radiation at 35 kV, 30 mA in a 2 θ range of 5° to 80° with a step-size of 0.02° and a count time of 2 s/step. The specific surface areas were measured by N₂ adsorption using a Micromeritics ASAP 2420 analyzer and a multipoint BET method. The morphology and the particles size of the different supports were characterized using Field Emission Gun Scanning Transmission Electron Microscopy (FEG-STEM) on a JEOL JSM7100F instrument. The Pd and Cu content of the catalysts and their distribution were determined using Energy Dispersive Spectroscopy (EDS) on an EDAX SDD operating at 20 kV equipped with an SDD Apollo X detector. Fourier Transform Infra-Red (FTIR) Spectroscopy on a Jasco FT/IR-6300 was used to analyze the chemical bonds and the functional groups grafted onto the nanotubes. The particle size distribution of the MWCNTs before and after functionalization was analyzed using the Partica LA-950V2 laser scattering particle size distribution analyzer.

2.5 Nitrate Reduction

Reduction experiments have been carried out in a glass reactor, equipped with a magnetic stirrer at room temperature and atmospheric pressure, using hydrogen as the reducing agent and at a pH that varied with the type of support. In a typical run, 25 mg of catalyst was added to a reactor containing 50 mL of sodium nitrate (NaNO₃) solution (30 mg/L NO₃⁻) in demineralized water, which was then flushed with H₂ to remove air while being continuously stirred. At the end of the reaction (15 min or 120 min), the solution was filtered with 0.45 μ m micro-filter paper, and the filtrate was colorized for nitrate determination, which was done using a U-2900 Diodes Array UV-Vis spectrophotometer [44].

2.6 Determination of Nitrate Concentration

Beer-Lambert law states that a solution's absorbance is directly proportional to the concentration of the absorbing species it contains. Thus, UV/Vis spectroscopy can be used to determine the concentration of the absorbing species. An alternative to plotting calibration curves is to make use of the relationship:

$$C = k A \quad [1]$$

where C is the concentration of the unknown, A is the measured absorbance of the unknown, and k is a factor derived from the reference or standard solution. A plot of absorbance against concentration will be linear in a certain domain of concentration, and, thus, the concentrations of nitrate can be determined by comparison with the calibration curve.

3. Results and Discussion

3.1 Catalyst Characterization

Figure 1 shows the XRD pattern of the MWCNTs (after functionalization), AC, and titania. The MWCNTs pattern has typical peaks at 25.9° and 42.7°, corresponding to the graphite (002) and (100) planes [48], respectively, indicating a pristine structure. While the typical peaks at 24° and 42° in the AC pattern correspond to the (002) and (100) planes of activated carbon, respectively [49], their broad widths show that the AC is in an amorphous state. Two phases that can be attributed to titania (anatase (80.5%) and rutile (19.5%)) can be seen in the titania pattern. Figure S1 shows the XRD patterns of the functionalized MWCNTs and Pd-Cu catalyst deposited on the functionalized MWCNTs. The peaks typical of pristine graphite are again present at 25.9° (reflection 002) and 42.7° (reflection 100). There are also peaks at 40.1° and 46.7° corresponding to the reflection planes (111) and (200), respectively of crystalline Pd with a face centered cubic structure (fcc) [50]. However, there is no clear peak that can be attributed to Cu, which would be expected to appear at 43°, corresponding to the reflection of the (111) plane. This may be due to the low percentage of Cu and/or by overlapping with the graphite peak at 42.7°.

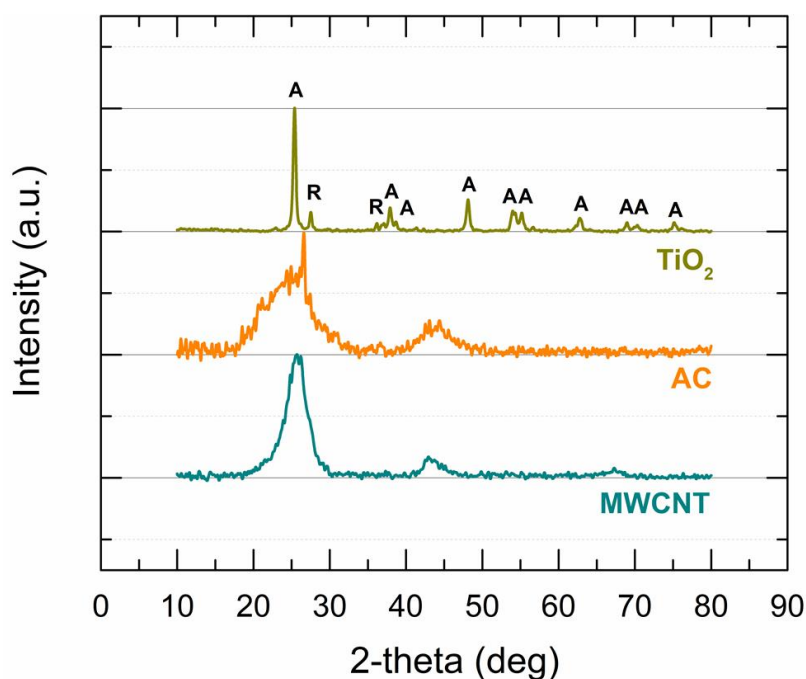


Figure 1 XRD patterns of the MWCNTs, AC, and Titania; A: *Anatase*, R: *Rutile*.

Surface modification of the MWCNTs with HNO_3 solution was investigated by FTIR to confirm the formation of the functional groups on the surface of the MWCNTs. The results are shown in Figure 2(a). The peak at 1430 cm^{-1} can be assigned to C=C asymmetric stretch [51], while the C-OH stretching mode can be found at 3430 cm^{-1} and the stretching vibration of the C=O double bond can be found close to 1710 cm^{-1} . The peaks at 1710 cm^{-1} and 3430 cm^{-1} , corresponding to the C=O of carboxylic acid and the OH hydroxyl group, indicate oxidation of carbon atoms on the surface of the MWCNTs by the HNO_3 . For comparison, figure 2(b) shows the FTIR spectrum of the AC. The peak at about 3440 cm^{-1} can be assigned to the O-H stretching mode of hydroxyl groups, the band at about 1700 cm^{-1} to C=O stretching vibrations of ketones, aldehydes, lactones or carboxyl groups, the broad band at $1000\text{-}1300\text{ cm}^{-1}$ to C-O stretching in acids, alcohols, phenols, ethers and esters groups; and the peak at 1430 cm^{-1} to C=C asymmetric stretch.

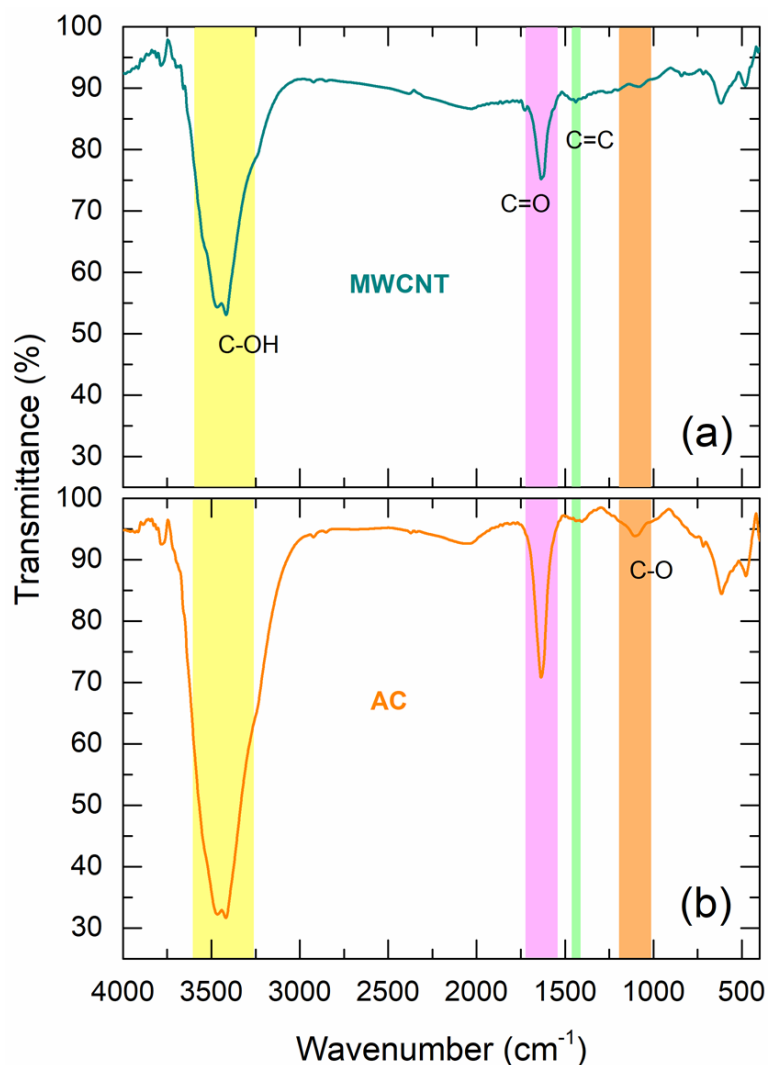


Figure 2 FT-IR spectra of (a) the functionalized MWCNTs, and (b) AC.

The evolution of the particle size distribution of MWCNTs during sonication in 8 M HNO₃ solution and after refluxing in 3 M HNO₃ solution is shown in Figure 3. The dispersion of the MWCNTs is noticeably enhanced after 1 h of sonication; however, there is little further increase in dispersion when the sonication period is increased to 3 h. Compared to the sonication process, refluxing seems to be less effective in decreasing the size of the MWCNT particles. And the sizes remain micrometric in both cases, which is due to the length of the carbon nanotubes.

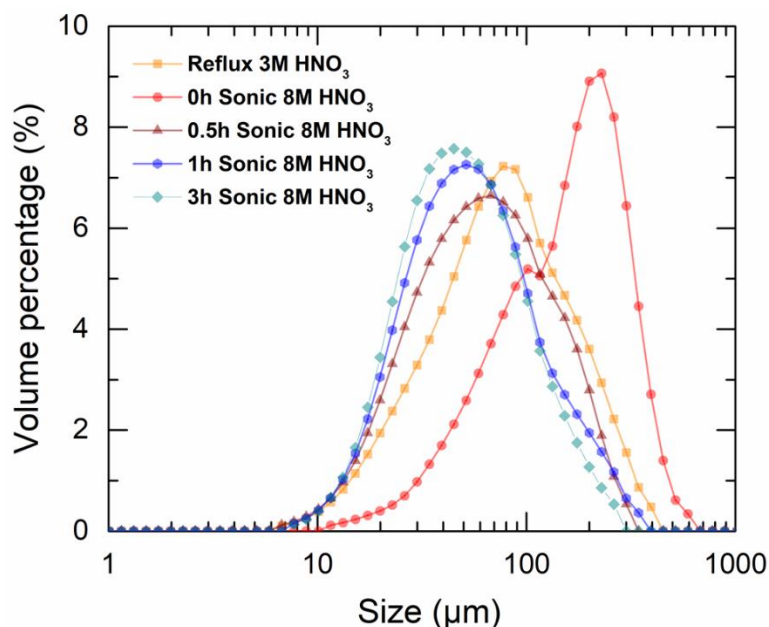


Figure 3 Particle size distribution of the MWCNTs functionalized using two different approaches - sonification and refluxing.

SEM micrographs of the as-received MWCNTs, purified MWCNTs, titania, and activated carbon are shown in Figure 4. Curved MWCNTs with a cylindrical shape are visible in the as-received MWCNTs (Figure (4-a)). The cylindrical shape of the MWCNTs, with a nanometric diameter size and micrometric length, becomes more obvious following the purifying step at 350°C (Figure (4-b)). The surface morphology of the TiO₂ (Figure 4-c) shows a uniform and homogeneous distribution of spherical TiO₂ particles with nanometric size. The activated carbon image reveals particles with micrometric sizes (Figure 4-d). At this magnification, the surface of the AC, which is usually full of irregular cavities that can serve as the main channels to connect to the inner and outer surfaces of the AC, is not well-resolved. Energy-dispersive X-ray spectroscopy (EDS) was used to provide qualitative and semi-quantitative information about the elemental composition of the surface of the catalysts. The EDS spectra are given in supporting information (see Figures S1-S3). The results show that Pd and Cu are present on the surface of all three prepared catalysts.

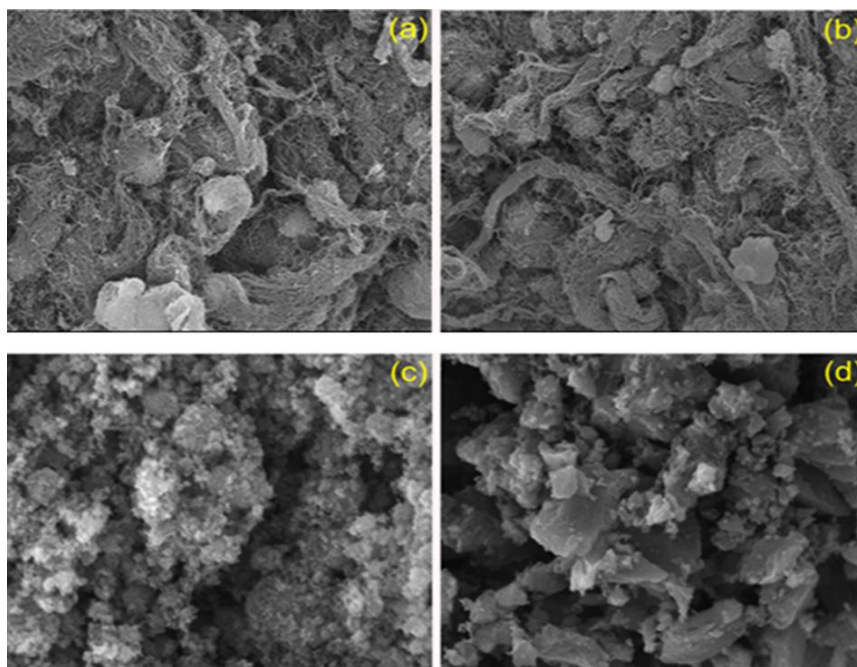


Figure 4 Scanning Electron Microscopy (SEM) images of: (a) MWCNTs as-received; (b) Purified MWCNTs; (c) TiO₂; and (d) AC.

To further analyze the morphology of bimetallic Pd-Cu catalysts, TEM of Pd-Cu/MWCNTs was carried out, as shown in Figure 5. Supported active metal particles on the MWCNTs are visible in the TEM images. The EDX elemental mappings of Pd-Cu nanoparticles on the MWCNTs show the dispersion of each metal (Pd and Cu) on the surface of the MWCNTs. This shows that the Cu is dispersed homogeneously, while some of the Pd is present in agglomerations on the surface of the support (Figure S4 in the supporting information).

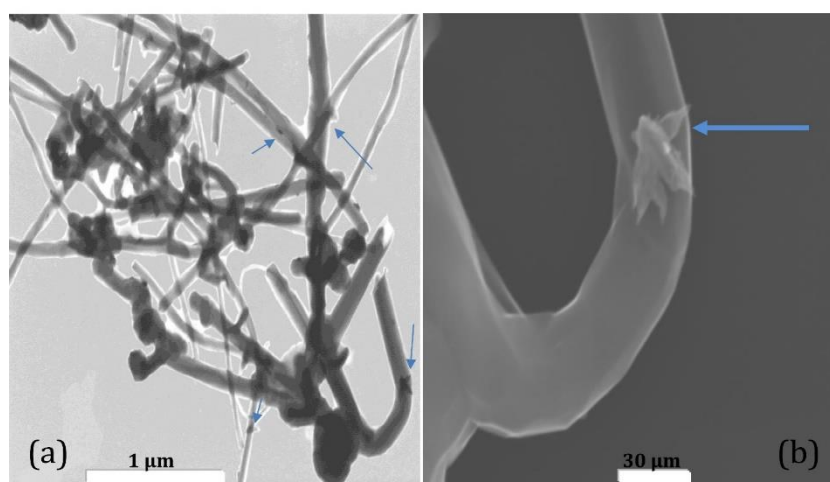


Figure 5 TEM micrographs of the Pd-Cu/MWCNTs: a) 1 μm resolution and b) 100 μm resolution.

Table 1 summarizes the BET surface areas and the pores volumes of the supports used in this study. The activated carbon support presents both the highest BET surface area and the highest total pore volume. Titania shows the lowest BET surface area and the lowest mesoporous surface

area, while MWCNTs show the highest BET mesopore surface area. These differences can, in part, be attributed to the absence of micropores in both TiO₂ and the MWCNTs. To confirm the specific surface area of the samples, N₂ adsorption-desorption isotherms were performed. The MWCNTs and TiO₂ isotherms (Figures 6a and 6c, respectively) are of type IV, characteristic of mesoporous materials with a finite multilayer formation followed by capillarity condensation. At the same time, the AC isotherm (Figure 6b) is of type I, characteristic of microporous materials. The hysteresis loops of the MWCNTs and TiO₂ are close to the H1 type, which corresponds to materials with cylindrical pore geometry and high pore size uniformity. While for the AC, the hysteresis loop is of the H4 type, characteristic of narrow slit-like pores.

Table 1 Texture properties of the supports.

Support	S _{BET} (m ² /g)	V _{micro} (cm ³ /g)	S _{meso} (m ² /g)	V _{total} (cm ³ /g)
Functionalized MWCNTs	250	0	264	1,59
AC	837	0.32	88	0.50
TiO ₂	53	0	57	0.50

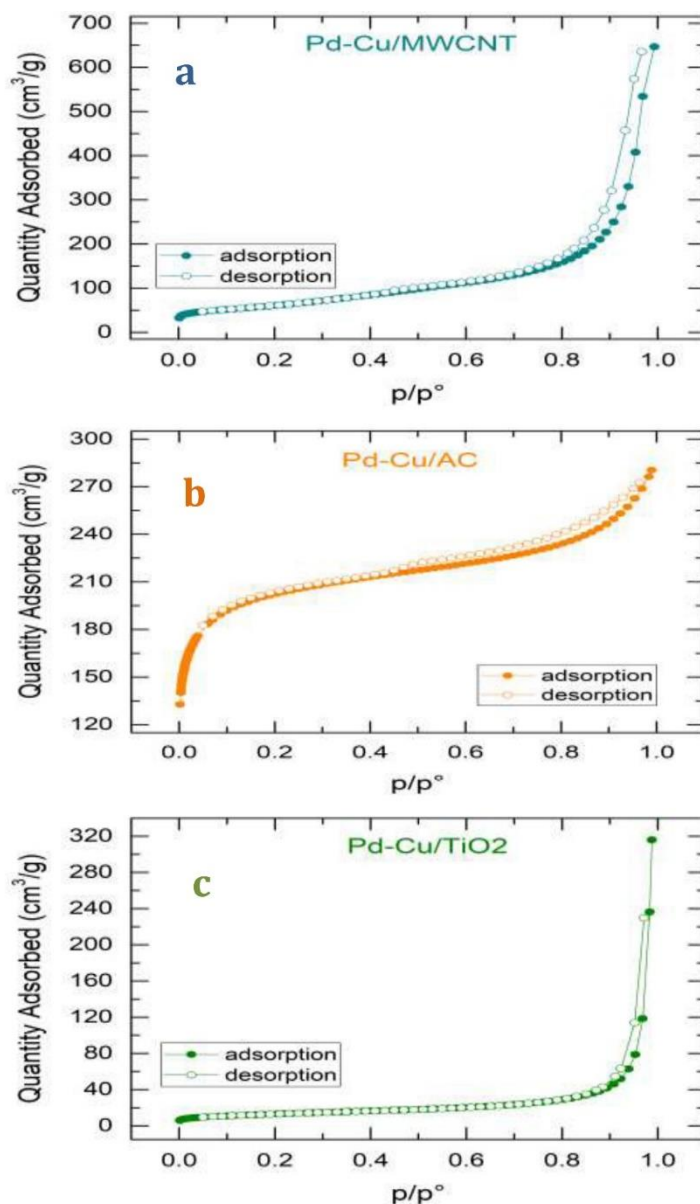


Figure 6 Nitrogen adsorption-desorption isotherms for: (a) Pd-Cu/MWCNTs; (b) Pd-Cu/AC; and (c) Pd-Cu/TiO₂.

3.2 Catalytic Reduction of Nitrate

3.2.1 Effect of the Support

To study the influence of the support on the performance of nitrate reduction catalysts, catalytic reduction experiments were performed using all three supported bimetallic catalysts (Pd-Cu/MWCNTs, Pd-Cu/AC, and Pd-Cu/TiO₂). The degree of nitrate conversion after 2 h of the reaction using each of these three supports is shown in Figure S5. All experiments were carried out with $C_{\text{NO}_3^-} = 30$ ppm, $C_{\text{catalyst}} = 0.5$ g/L, and $\text{pH} = 7$. The results show that the MWCNTs-supported catalyst had the best performance, with a nitrate conversion rate of more than 98%. Titania also shows a high nitrate conversion rate (88.7%). However, for the activated carbon, the performance was moderate at best (43%).

The differences in performance can be related to the surface chemistry of each support. For carbon material supports, MWCNTs have advantages over activated carbon, as aggregates of the tubes can act as mesoporous materials with the active metal sites located on the outer walls of the tubes, thus, avoiding the mass transfer limitations common in porous materials such as activated carbon that will decrease the apparent activity and even modify the selectivity of the catalyst [52]. The limitation of mass transfer in AC stems from the fact that most of the adsorption occurs in its micropores, only a few of which are located on the outer surface, with mesopores and macropores acting as channels for the adsorbate into the inner micropores. This interpretation is supported by the BET analysis, as shown in Table 1. Although the activated carbon has the highest BET surface area and the highest total pore volume, it shows the lowest catalytic activity. This is due to the low number of mesopores (low mesopore surface area). In contrast, the high catalytic activity of carbon nanotubes can be attributed to the high numbers of mesopores and the absence of micropores. The presence of specific metal-support interactions may also affect the catalytic activity. The presence of oxygen and hydrogen in the surface groups has a great influence on the adsorption properties of activated carbons, while the random arrangement of incomplete aromatic sheets can lead to incompletely saturated valence states and unpaired electrons, affecting their adsorption behavior [53]. The fact that MWCNTs have a highly oriented structure results in them possessing better adsorption properties after being functionalized.

The good performance shown by Titania can be explained by the nature of the interaction between the metal nanoparticles and the TiO_2 support. Anatase TiO_2 is frequently used as a catalyst support for metal heterogeneous catalysts due to its strong interaction with metal nanoparticles. The XRD pattern of the Titania used in this study shows that it is 80.5% anatase. Although TiO_2 presents the lowest BET surface area and the lowest mesopore surface area, it presents higher catalytic activity than activated carbon. This can be explained by the mechanism proposed by Sá and Anderson [30], in which, in the case of bimetallic catalysts, nitrate adsorption occurs not only on the transition metals but also on the support. It has been proposed that nitrate, after the exchange with OH^- , may be adsorbed on the Lewis acid sites of TiO_2 and reduced by an electron-rich titania species (presumably Ti_4O_7) formed from hydrogen spillover, which leads to the formation of nitrites.

3.2.2 Effect of pH

The effect of varying the pH on the nitrate conversion rates of the three supported catalysts was studied while keeping $C_{\text{NO}_3^-} = 30\text{ppm}$ and $C_{\text{catalyst}} = 0.5\text{ g/L}$. The results are shown in Figure S5.

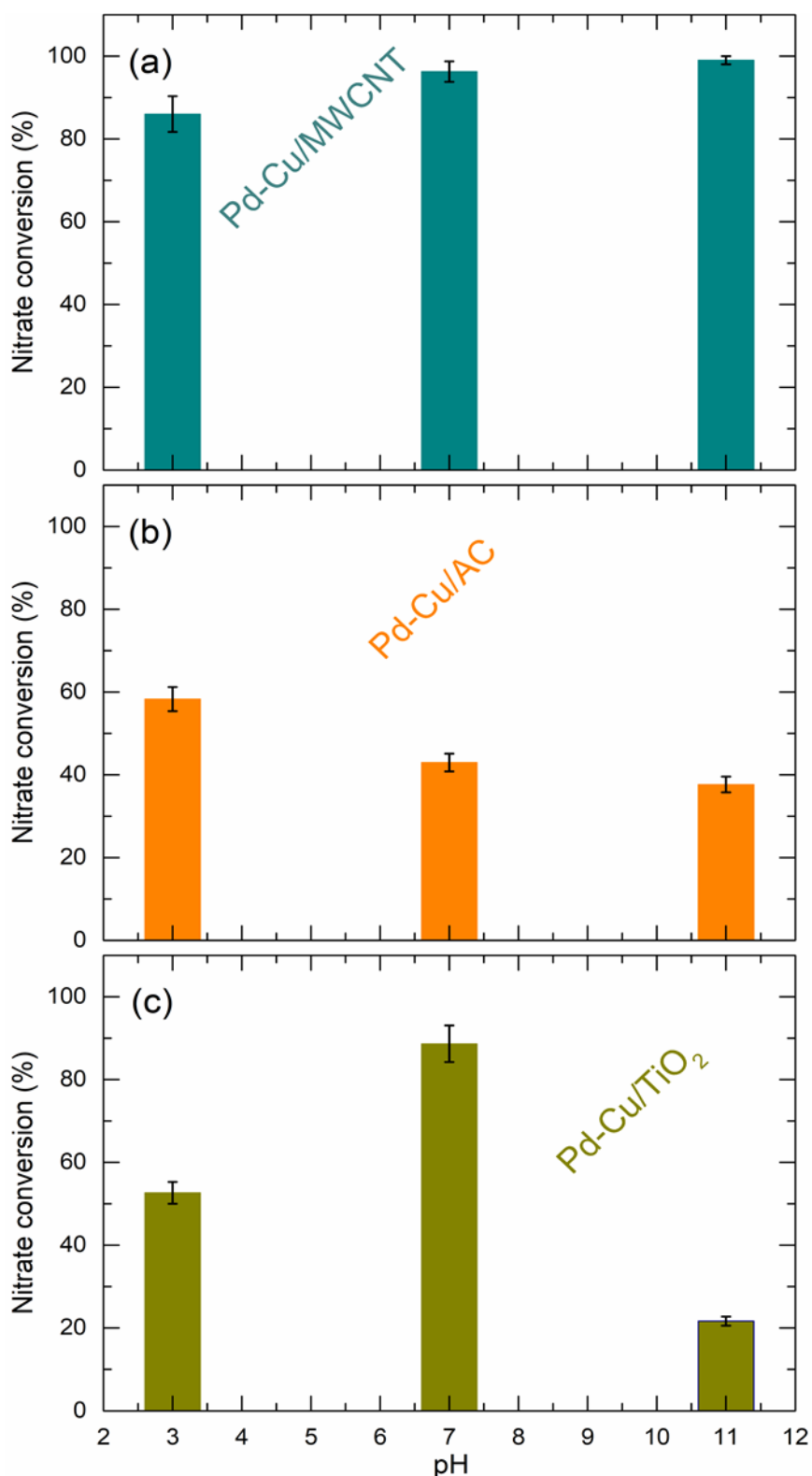


Figure 7 Nitrate conversion (%) after 2 h of catalytic reduction using a) Pd-Cu/MWCNTs, b) Pd-Cu/Activated Carbon, and c) Pd-Cu/TiO₂ as catalysts at a range of pH ($C_{NO_3^-} = 50$ ppm, $C_{catalyst} = 0.5$ g/L).

For Pd-Cu/MWCNTs (Figure 7-a), the catalytic activity significantly decreases in an acidic medium. Muataz et al. [54] reported that the point of zero charge “pH_{PZC}” of the MWCNTs is 6.6 drops from 6.6 to 3.1 after being functionalized with the carboxylic functional group. Hence, in an acidic

medium, the pH is almost equal to that of the point of zero charge (3.1), leading to the neutralization of the surface charge. The resulting agglomeration of carbon nanotubes can lead to a decrease in catalytic activity. It is also possible that, at certain pH, this support might be involved in the nitrate reduction mechanism.

Pd-Cu/TiO₂ (Figure 7-b) shows a decrease in the catalytic activity in a basic medium. According to Sá et al. [15], nitrates adsorb onto exposed Lewis acid sites (oxygen vacancies) of the support via electrostatic interactions. Electrons associated with the reduction process can therefore be found on Ti²⁺ centers, and, thus, nitrate reduction decreases at basic pH due to inhibitory binding of hydroxide ions at these centers at high pH.

The effect of activated carbon surface chemistry is clearly pH-dependent (Figure 7-c). The different interactions of the oxygenated groups found on its surface (carbonyls, hydroxyls, lactones, pyrone, and quinone) in acidic and basic mediums determine the surface charge of the AC and thus its activity in the reduction of nitrate. At high pH (pH > p*H*_{PZC}), the low absorption is due to electrostatic repulsion between the negatively charged carbon surface and nitrate anions. The improved catalytic activity in an acidic medium can be explained by the fact that the surface is positively charged, which promotes the absorption of nitrate ions [55].

4. Conclusions

The catalytic reduction of nitrates in water by the bimetallic catalyst Pd-Cu on three different supports (MWCNTs, AC, and Titania) has been studied. The highest catalytic performance in a neutral pH medium was observed by using MWCNTs as the support, with nitrate conversion of up to 99%. The effect of pH on the surface chemistry of the catalyst was found to have a great influence on their activity, with Pd-Cu/MWCNTs showing better catalytic performance in a basic medium, Pd-Cu/AC better performance in an acidic medium, and Pd-Cu/Titania better performance in a neutral pH medium. These results show that it is very important to select support according to the practical conditions to efficiently reduce nitrate ions in aqueous solutions.

Author Contributions

Mouhamad Rachini, PhD Student (Formal analysis: Equal; Investigation: Supporting; Methodology: Supporting; Validation: Equal; Writing – original draft: Supporting). Mira Jaafar, PhD (Conceptualization: Equal; Formal analysis: Equal; Investigation: Supporting; Methodology: Supporting; Validation: Supporting; Writing – original draft: Supporting). Zahraa Sleiman, PhD Student (Formal analysis: Equal; Supervision: Equal; Investigation: Supporting; Methodology: Supporting; Validation: Equal; Writing – original draft: Supporting). Mohammad Kassem, PhD (Conceptualization: Equal; Supervision: Equal; Formal analysis: Equal; Investigation: Supporting; Methodology: Supporting; Validation: Supporting; Writing – original draft: Supporting). Eugene Bychkov, Prof, PhD, HDR (Conceptualization: Equal; Formal analysis: Equal; Investigation: Supporting; Methodology: Supporting; Project administration: Supporting; Supervision: Equal; Validation: Equal; Writing – original draft: Supporting). T. Jean Daou, Prof, PhD, HDR (Conceptualization: Equal; Formal analysis: Equal; Investigation: Supporting; Methodology: Supporting; Project administration: Supporting; Supervision: Equal; Validation: Equal; Writing – original draft: Supporting). Joumana Toufaily, Prof, PhD, HDR (Conceptualization: Equal; Formal analysis: Equal; Funding acquisition: Supporting; Investigation: Supporting; Methodology:

Supporting; Resources: Equal; Validation: Equal; Writing – original draft: Supporting). Tayssir Hamieh, PhD, HDR, ENG (Conceptualization: Equal; Formal analysis: Equal; Funding acquisition: Equal; Investigation: Lead; Methodology: Lead; Project administration: Lead; Resources: Equal; Supervision: Equal; Validation: Equal; Writing–original draft: Lead; Writing – review & editing: Lead).

Competing Interests

The authors declare that they have no known competing financial interests or personal relationships that could have appeared to influence the work reported in this paper.

Additional Materials

The following additional materials are uploaded at the page of this paper.

1. Figure S1: EDX pattern of Pd-Cu/ MWCNTs.
2. Figure S2: EDX pattern of Pd-Cu/TiO₂.
3. Figure S3: EDX pattern of Pd-Cu/AC.
4. Figure S4: EDX elemental mappings of Pd-Cu nanoparticles on MWCNTs.
5. Figure S5: Nitrate conversion (%) after 2 h of catalytic reduction using different supports ($C_{NO_3^-} = 30 \text{ ppm}$, $C_{catalyst} = 0.5 \text{ g/L}$, $pH = 7$)

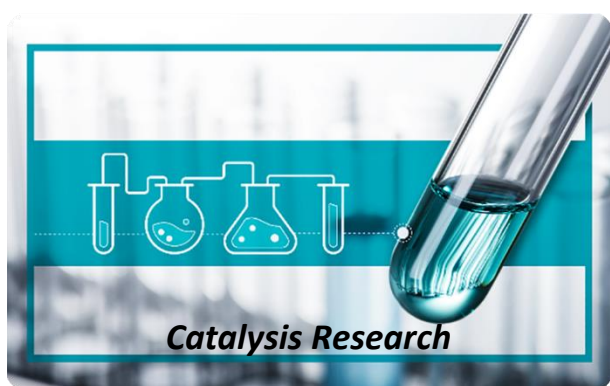
References

1. Fan AM, Steinberg VE. Health implications of nitrate and nitrite in drinking water: An update on methemoglobinemia occurrence and reproductive and developmental toxicity. *Regul Toxicol Pharmacol.* 1996; 23: 35-43.
2. World Health Organization (W.H.O). Guidelines for drinking-water quality. 4th ed. World Health Organization: Switzerland; 2004. pp. 398-403.
3. U.S. Geological Survey Web Site (USGS). Nitrogen and Water [Internet]. Available from: https://www.usgs.gov/special-topic/water-science-school/science/nitrogen-and-water?qt-science_center_objects=0#qt-science_center_objects.
4. Gray FN. Drinking water quality problems and solutions. 2nd Edition. Cambridge University Press; 2008. pp. 538.
5. Schick J, Daou TJ, Caultet P, Paillaud JL, Patarin J, Mangold Callare C. Surfactant-modified MFI nanosheets: A high capacity anion-exchanger. *Chem Commun.* 2011; 47: 902-904.
6. Rautenbach R, Kopp W, Van Opbergen G, Hellekes R. Nitrate reduction of well water by reverse osmosis and electrodialysis - studies on plant performance and costs. *Desalination.* 1987; 65: 241-258.
7. Häyrynen K, Pongrácz E, Väisänen V, Papa N, Mänttari M, Langwaldt J, et al. Concentration of ammonium and nitrate from mine water by reverse osmosis and nanofiltration. *Desalination.* 2009; 240: 280-289.
8. El Midaoui A, Elhannouni F, Taky M, Chay L, Sahli MAM, Echihabi L, et al. Optimization of nitrate removal operation from ground water by electrodialysis. *Sep Purif Technol.* 2002; 29: 235-244.
9. El Hanache L, Lebeau B, Nouali H, Toufaily J, Hamieh T, Daou TJ. Performance of surfactant-modified *BEA-type zeolite nanosponges for the removal of nitrate in contaminated water:

- Effect of external surface. *J Hazard Mater.* 2019; 364: 206-217.
10. El Hanache L, Sundermann L, Lebeau B, Toufaily J, Hamieh T, Daou TJ. Surfactant-modified MFI-type nanozeolites: Super-adsorbents for nitrate removal from contaminated water. *Micro Meso Mater.* 2019; 283: 1-13.
 11. Kapoor A, Viraraghavan T. Nitrate removal from drinking water. *J Environ Eng.* 1997; 123: 371-380.
 12. Vorlop K, Tacke T. First steps towards the removal of nitrate and nitrite from drinking water with noble metal catalysts. *Chem Eng Technol.* 1989; 61: 836-837.
 13. Gao W, Guan N, Chen J, Guan X, Guan X, Jin R, et al. Titania supported Pd-Cu bimetallic catalyst for the reduction of nitrate in drinking water. *Appl Catal B.* 2003; 46: 341-351.
 14. Epron F, Gauthard F, Barbier J. Catalytic reduction of nitrate in water on a monometallic Pd/CeO₂ catalyst. *J Catal.* 2002; 206: 363-367.
 15. Sá J, Berger T, Föttinger K, Riss A, Anderson JA, Vinek H. Can TiO₂ promote the reduction of nitrates in water? *J Catal.* 2005; 234: 282-291.
 16. Prüsse U, Vorlop KD. Supported bimetallic palladium catalysts for waterphase nitrate reduction. *J Mol Catal A Chem.* 2001; 173: 313-328.
 17. Deganello F, Liotta LF, Macaluso A, Venezia AM, Deganello G. Catalytic reduction of nitrates and nitrites in water solution on pumice-supported Pd-Cu catalysts. *Appl Catal B Environ.* 2000; 24: 265-273.
 18. Ilinitch OM, Nosova LV, Gorodetskii VV, Ivanov VP, Trukhan SN, Gribov EN, et al. Catalytic reduction of nitrate and nitrite ions by hydrogen: Investigation of the reaction mechanism over Pd and Pd-Cu catalysts. *J Mol Catal A Chem.* 2000; 158: 237-249.
 19. Epron F, Gauthard F, Pinéda C, Barbier J. Catalytic reduction of nitrate and nitrite on Pt-Cu/Al₂O₃ catalysts in aqueous solution: Role of the interaction between copper and platinum in the reaction. *J Catal.* 2001; 198: 309-318.
 20. Gauthard F, Epron F, Barbier J. Palladium and platinum-based catalysts in the catalytic reduction of nitrate in water: Effect of copper, silver, or gold addition. *J Catal.* 2003; 220: 182-191.
 21. Gholinejad M, Khosravi F, Afrasi M, Sansano JM, Nájera C. Applications of bimetallic PdCu catalysts. *Catal Sci Technol.* 2021; 11: 2652-2702.
 22. Gholinejad M, Bahrami M, Nájera C, Pullithadathil B. Magnesium oxide supported bimetallic Pd/Cu nanoparticles as an efficient catalyst for Sonogashira reaction. *J Catal.* 2018; 363: 81-91.
 23. Lemaigen L, Tong C, Begon V, Burch R, Chadwick D. Catalytic denitrification of water with palladium-based catalysts supported on activated carbons. *Catal Today.* 2002; 75: 43-48.
 24. Mikami I, Sakamoto Y, Yoshinaga Y, Okuhara T. Kinetic and adsorption studies on the hydrogenation of nitrate and nitrite in water using Pd-Cu on active carbon support. *Appl Catal B Environ.* 2003; 44: 79-86.
 25. Sá J, Gasparovicova D, Hayek K, Halwax E, Anderson JA, Vinek H. Water denitration over a Pd-Sn/Al₂O₃ catalyst. *Catal Lett.* 2005; 105: 209-217.
 26. Pintar A, Batista J, Levec J. Catalytic denitrification: Direct and indirect removal of nitrates from potable water. *Catal Today.* 2001; 66: 503-510.
 27. Sá J, Vinek H. Catalytic hydrogenation of nitrates in water over a bimetallic catalyst. *Appl Catal B Environ.* 2005; 57: 247-256.
 28. Garron A, Lazar K, Epron F. Effect of the support on tin distribution in Pd-Sn/Al₂O₃ and PdSn/SiO₂ catalysts for application in water denitration. *Appl Catal B Environ.* 2005; 59: 57-69.

29. Marchesini FA, Irusta S, Querini C, Miro E. Nitrate hydrogenation over Pt,In/Al₂O₃ and Pt,In/SiO₂. Effect of aqueous media and catalyst surface properties upon the catalytic activity. *Catal Commun.* 2008; 9: 1021-1026.
30. Sá J, Anderson JA. FTIR study of aqueous nitrate reduction over Pd/TiO₂. *Appl Catal B Environ.* 2008; 77: 409-417.
31. Barrabés N, Just J, Dafinov A, Medina F, Fierro JLG, Sueiras JE, et al. Catalytic reduction of nitrate on Pt-Cu and Pd-Cu on active carbon using continuous reactor - the effect of copper nanoparticles. *Appl Catal B Environ.* 2006; 62: 77-85.
32. Sakamoto Y, Kanno M, Okuhara T, Kamiya Y. Highly selective hydrogenation of nitrate to harmless compounds in water over copperpalladium bimetallic clusters supported on active carbon. *Catal Lett.* 2008; 125: 392-395.
33. Gavagnin R, Biasetto L, Pinna F, Strukul G. Nitrate removal in drinking waters: The effect of tin oxides in the catalytic hydrogenation of nitrate by Pd/SnO₂ catalysts. *Appl Catal B Environ.* 2002; 38: 91-99.
34. Gasparovicova D, Kralik M, Hronec M, Vallusova Z, Vinek H, Corain B. Supported Pd-Cu catalysts in the water phase reduction of nitrates: Functional resin versus alumina. *J Mol Catal A Chem.* 2007; 264: 93-102.
35. Xu Z, Chen L, Shao Y, Yin D, Zheng S. Catalytic hydrogenation of aqueous nitrate over Pd-Cu/ZrO₂ catalysts. *Ind Eng Chem Res.* 2009; 48: 8356-8363.
36. Strukul G, Gavagnin R, Pinna F, Modaferrri E, Perathoner S, Centi G, et al. Use of palladium based catalysts in the hydrogenation of nitrates in drinking water: From powders to membranes. *Catal Today.* 2000; 55: 139-149.
37. Yoshinaga Y, Akita T, Mikami I, Okuhara T. Hydrogenation of nitrate in water to nitrogen over Pd-Cu supported on active carbon. *J Catal.* 2002; 207: 37-45.
38. Soares OSGP, Órfão JJM, Pereira MFR. Nitrate reduction in water catalyzed by Pd-Cu on different supports. *Desalination.* 2011; 279: 367-374.
39. Rodríguez Reinoso F. The role of carbon materials in heterogeneous catalysis. *Carbon.* 1998; 36: 159-175.
40. Soares SOGP, Órfão JJM, Pereira MFR. Pd-Cu and Pt-Cu catalysts supported on carbon nanotubes for nitrate reduction in water. *Ind Eng Chem Res.* 2010; 49: 7183-7192.
41. Yoon B, Pan HB, Wai CM. Relative catalytic activities of carbon nanotube-supported metallic nanoparticles for room-temperature hydrogenation of benzene. *J Phys Chem C.* 2009; 113: 1520-1525.
42. Serp P, Castillejos E. Catalysis in carbon nanotubes. *Chemcatchem.* 2010; 2: 41-47.
43. Tokazhanov G, Ramazanov E, Hamid S, Bae S, Lee W. Advances in the catalytic reduction of nitrate by metallic catalysts for high efficiency and N₂ selectivity: A review. *Chem Eng J.* 2020; 384: 123252.
44. Job N, Heinrichs B, Léonard A, Colomer JF, Marien J, Pirard JP. Avoiding mass transfer limitation on carbon supported catalysis by using carbon xerogel as supports. *Chem Sustainable Dev.* 2006; 14: 571-575.
45. Ruiz MP, Faria J, Shen M, Drexler S, Prasomsri T, Resasco DE. Nanostructured carbon-metal oxide hybrids as amphiphilic emulsion catalysts. *ChemSusChem.* 2011; 4: 964-974.
46. Abdelbaki R, Bouguettoucha A, Chebli D, Amrane A. Adsorption of ethyl violet dye in aqueous solution by forest wastes, wild carob. *Desalin Water Treat.* 2016; 57: 9859-9870.

47. Calahorra FJ, Extramiana J, de la Rosa F, Díaz González R, Leiva O, Borobia V. Bladder hernias. *Actas Urol Esp.* 1986; 10: 505-508.
48. Ganiyu SA, Tanimu A, Azeez MO, Alhooshani K. Hierarchical porous nitrogen-doped carbon modified with nickel nanoparticles for selective ultradeep desulfurization. *ChemistrySelect.* 2020; 5: 8483-8493.
49. Naoe K, Kataoka M, Kawagoe M. Preparation of water-soluble palladium nanocrystals by reverse micelle method: Digestive ripening behavior of mercaptocarboxylic acids as stabilizing agent. *Colloids Surf A Physicochem Eng Asp.* 2010; 364: 116-122.
50. Dai YM, Pan TC, Liu WJ, Jehng JM. Highly dispersed Ag nanoparticles on modified carbon nanotubes for low-temperature CO oxidation. *Appl Catal B Env.* 2011; 103: 221-225.
51. Soares OSGP, Órfão JJM, Pereira MFR. Bimetallic catalysts supported on activated carbon for the nitrate reduction in water: Optimization of catalysts composition. *Appl Catal B Env.* 2009; 91: 441-448.
52. Atieh MA, Bakather OY, Al Tawbini B, Bukhari AA, Abuilawi FA, Fettouhi MB. Effect of carboxylic functional group functionalized on carbon nanotubes surface on the removal of lead from water. *Bioinorg Chem Appl.* 2010; 2010: 603978.
53. Badosz TJ. Surface chemistry of carbon materials. In: *Carbon materials for catalysis.* John Wiley and Sons: Hoboken; 2009. pp. 45-92.
54. Iida T, Amano Y, Machida M, Imazeki F. Effect of surface property of activated carbon on adsorption of nitrate ion. *Chem Pharm Bull.* 2013; 61: 1173-1177.
55. Chungsyng L, Chiu H. Adsorption of zinc (II) from water with purified carbon nanotubes. *Chem Eng Sci.* 2006; 61: 1138-1145.



Enjoy *Catalysis Research* by:

1. [Submitting a manuscript](#)
2. [Joining in volunteer reviewer bank](#)
3. [Joining Editorial Board](#)
4. [Guest editing a special issue](#)

For more details, please visit:

<http://www.lidsen.com/journals/cr>